MŰEGYETEM 1782

Hygrothermal Behavior of Modern Masonry Building Constructions

Book of Theses

Balázs Nagy

Supervisor: Dr. habil György Mihály Stocker

Budapest University of Technology and Economics, Faculty of Civil Engineering,
Department of Constrution Materials and Technologies

Budapest, 2019

TABLE OF CONTENTS

I. INTRODUCTION

1. Motivation

Buildings sector (residential and commercial buildings) represents 30% the of the total energy use worldwide, and also almost 40% of the total direct and indirect CO_2 emissions in 2017. Beside this, constructions are responsible for additional 6% of total energy use. Furthermore, energy consumption in buildings worldwide is predicted to be increased by an average of 1.5%/year from 2012 to 2040 [1]. Therefore, thermal insulation of new and existing buildings is an extremely important field in this sector, since it helps reduce the energy demand and decrease carbon emissions [2]. According to EU's long-term goal the greenhouse gas emissions should be reduces by 80-95% by 2050, comparing to the level of 1990, [3]. This ambitious plan requires strict building regulations. According to the Energy Performance Building Directive (EPBD), member states of the EU must apply minimum requirements regarding the energy performance of new and existing buildings, and implement them into their building energy certifications [4]. A comprehensive review on energy policies can be found in [5]. The new legislation was introduced in 2006 in Hungary [6]. There are three levels of the key requirements: first one is the thermal transmittance (U value) of the building envelope, the second one is the specific heat loss coefficient (q value), and third one is the primary energy use of the building (E_p). The former two requirements depend only on the design and construction of the building and the quality of the thermal envelope. In recent years, there have been many changes in the field of building energetics, partly due to technical developments and partly to the change of the directives and regulations [7]. The requirements of energy performance certifications (EPC) of buildings have been constantly tightened in the EU [8] and also in Hungary [9], [10] in the past years, since the introduction of the recasted EPBD [11]; however this has not had significant effects yet on people's mind in the domestic property market. Most of the people do not care about the energy performance of their buildings and they see EPC as a new expression of bureaucracy [12], although, due to the performance evaluation of buildings [13] it is clearly visible, that people mostly live in buildings that need energy efficiency and performance improving refurbishments. In the Hungarian residential real estate market, almost one thing matters only, besides of location of the property: whether it is a panel or a brick building, how real estate firms typify the whole building sector [14]. The advantage of the stricter requirements is that they make thermal insulation of new and existing buildings inevitable, and push the industry toward energy efficiency. Current mandatory level of energy performance is called "cost-optimized" in Hungary and made according to the revised EPBD based on cost-optimum calculation of some typical Hungarian residential and non-residential buildings [15], [16]. These "cost-optimized" requirements are above "cost-optimum", mostly because of today's economic environment [17]; however, it still helps reduce CO_2 emission more, than previous requirements. In near future, when nearly zero energy buildings (NZEB) will be the new mandatory standard, the requirements will continue to be tighten; however, the domestic legislation made simpler choices possible than researchers, like Szalay and Zöld, whose proposals are based on large building samples [18], [19]. A comprehensive review of the cost-optimum analysis for NZEBs is presented by Ferrara et al [20] showing that the cost-optimized approach is an effective method for determining the future of NZEB planning across the EU. Speaking of Europe, it is inevitable to think about different climates when considering the energy requirements. Ahmed et al [21] presented a new method in contrast to NZEB requirements in different climates and countries. Countries like Greece have different climate zones for energy performance calculation, and researchers [22] showed that the energy efficiency measures of buildings should vary according to the four climate zones. Hungarian regulation considers the whole country as one climate zone, although it was shown previously that there could be more than 10% difference in climate related data [23].

In accordance with the above mentioned upcoming mandatory NZEB requirements, building materials, elements and constructions have been being developed significantly in the past few years. In the future, we can expect not only the high-tech, but conventional techniques to be improve with the use of environmentally-friendly materials and energy efficient technology [24]. Building material manufacturers have already started to develop new products to prepare for these requirements of near future. To achieve significant heat loss reduction of buildings, the demand is increased particularly for new insulations and development of new technical solutions. These new requirements have serious effects on the Hungarian masonry industry [25], which started developing and introducing new and reinvented products in the recent years [26], [27]. Brick manufacturers started to produce masonry blocks filled with thermal insulation material to increase the thermal resistance of bricks, and to sell insulation together with the masonry blocks. These blocks are used in new constructions across Central-Europe with different geometry and fillers; however, many of their properties, such as hygrothermal behavior is not yet researched in details neither the blocks, nor in building constructions.

Numerical simulation techniques developed amazingly in the past 30 years [28], in these days almost everything can be implemented and analyzed by computer modeling. Hundreds of building energy software have been developed or enhanced in the last decades [29], among them there are also tools that are capable to perform hygrothermal analysis. The performance of hygrothermal analysis depends immensely on the sophistication of mathematical models used, and also on the degree to which the model takes the dimensions, type of flow and quality of input data into consideration [30]. It is evident, that a multidimensional model is more accurate, than a one-dimensional one, and a dynamic model gives more sophisticated results than a steady-state one. However, without accurate input data, as material properties and boundary conditions, the results of numerical simulations will never approach the real behavior. It is also obvious, that dynamic and multidimensional modeling is not always necessary, there are certain situations (e.g. EPC), when simplified models should be used in order to be compatible with the existing, simplified calculation methods. Therefore, it is useful to define equivalent values, that can be used in simplified calculations.

In my PhD research, because of the above mentioned reasons, I investigated modern, insulation filled masonry blocks to understand their hygrothermal behavior in details, and its effects on their energy performance, to help masonry producers develop better products. I used detailed FEM based thermal and conjugated heat and moisture transport (HAM) modeling supported by laboratory measurements, in order to evaluate the performance of these blocks, and also to understand the hygrothermal behavior of walls and building constructions made of these blocks. I conducted steady state and dynamic simulations, and created new techniques and measures to analyze the conjugated heat and moisture behavior of these masonry products. I was very interested how considering hygrothermal approach effects on thermal and moisture transmittance and how these properties depend on climate.

2. **Research plan**

In my dissertation, I made comprehensive reviews on the available scientific literature in the topics of thermal and hygrothermal modelling of building constructions, including the brief history of heat and moisture transport, numerical tools for thermal and hygrothermal simulations and thermal and hygrothermal modeling of construction joints. I also reviewed the available scientific literature about the thermal and hygrothermal performance of modern hollow and filled masonry blocks. I also covered the topic of optimization studies of masonry block geometries. After reviewing the available literature, I selected the scope of my dissertation and formulated research questions.

The main objective of my dissertation is to get better understanding on the thermal and hygrothermal behavior of modern, thermal insulation filled masonry blocks. This interest of examining masonry blocks, among other things, is due to the fact that during my PhD research I was able to take part in a number of industrial work within the Laboratory of Building Physics that I had to deal with such masonry blocks. Other driving force was the money and infrastructure, or more specifically, its absence. Our laboratory is now in developing stage, and we have limited resources; however, I would like to be able to compete with research institutes that have been operating for a long time and with significantly higher financial resources.
The selected topics and the schematics of the research plan based on the selected topics is summarized in **Fig. 1**.

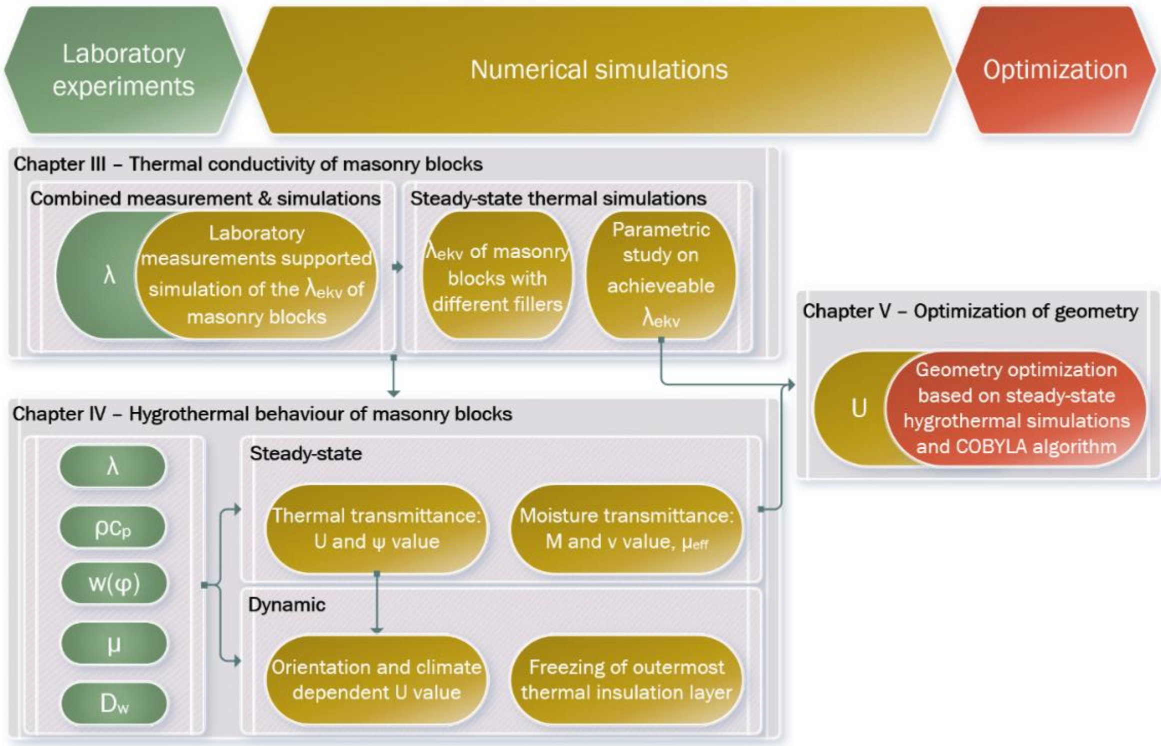

Fig. 1 Schematic of the research plan

II. MATERIALS AND METHODS

1. Materials of modern masonry structures

Parts of modern building blocks and masonry can be categorized in three main material groups. Fired clay, as the structure of the blocks, thermal insulation fillers, and mortar and plasters. As there is great number of possibilities for the selection of materials, in this dissertation, it was necessary to limit the scope of investigated materials.

1.1. Fired clay

During my PhD studies, I examined numerous fired clay samples and bricks in the Laboratory of Building Physics for industrial customers, manufactured in different Hungarian fired clay factories (e.g. Balatonszentgyörgy, Tiszavasvári). From these measured samples, which were cut-out and sanded plates from masonry blocks (see Error! Reference source not found. and **REF _Ref533692198 \h * MERGEFORMAT** Error! Reference source not found.), I selected the most common and therefore representative samples and used their measured and averaged values to evaluate the Hungarian fired clay.

1.2. Thermal insulations

Since 2014, I measured and analyzed more than 30 different insulations in the Laboratory of Building Physics, primarily in relation to their thermal conductivity, and in many cases I also examined hygrothermal properties, such as sorption isotherm, water vapor diffusion resistance factor, liquid transport coefficient and volumetric heat capacity. **Fig. 2** shows some thermal insulations under microscope, illustrating the diversity of the structures of thermal insulation materials. From the examined thermal insulations, I selected five materials for my research based on their hygrothermal properties. I used mineral wool made of basalt (MW), as general filler for masonry blocks provided by industrial partners. I also examined the hollow blocks without fillers, with aerogel (AG), polyurethane foam (PUR) as well as expanded perlite (EXP). However, later in my research, I skipped the unfilled masonry blocks due to their low thermal performance, and added expanded polystyrene (EPS) filler instead. During my research, I examined both non-hygric aerogel particle filled and hygric aerogel blanket (AG) filled masonry blocks, although only the results of the latter one are included in this dissertation.

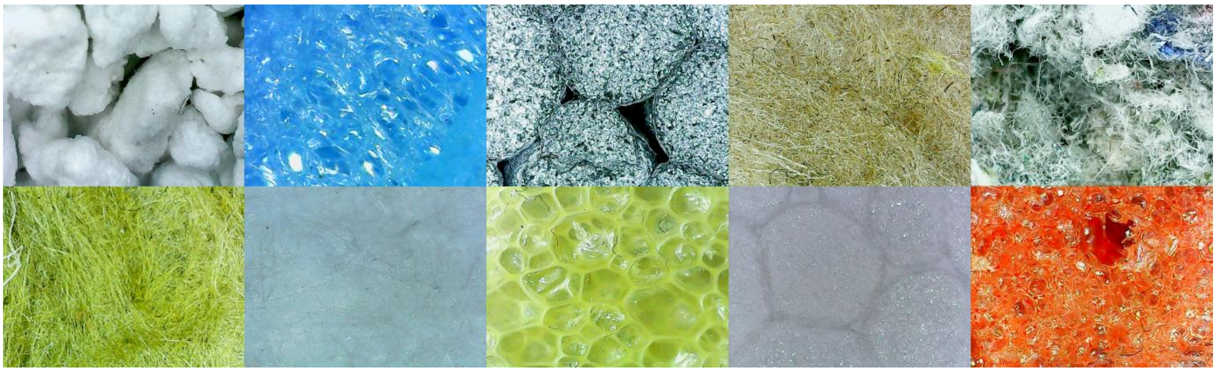

Fig. 2 Thermal insulations under microscope, from top left: expanded perlite, extruded polystyrene, expanded polystyrene with graphite, glass mineral wool, cellulose, rock mineral wool, aerogel blanket, polyurethane foam, expanded polystyrene and fire-resistant polyurethane foam

2. **Hygrothermal laboratory experiments**

2.1. *Thermal conductivity*

In the Laboratory of Building Physics of Department of Construction Materials and Technologies, for thermal conductivity and thermal resistance testing we use guarded hot plate method performed by Taurus TLP 300 DTX single guarded hot plate device. Thermal conductivity of building materials depends on its temperature, moisture content and age [31]–[34], the effects that can be taken into account by correction factors according to MSZ EN ISO 10456 [35].

2.2. Moisture storage curve

For composing moisture storage curves, adsorption isotherms of the materials were used. In the Laboratory of Building Physics, we measure sorption isotherms according to MSZ EN ISO 12571 [36] in self-made chambers by using salt solutions with internal air circulation system to reduce the surface moisture transfer resistance and therefore, fasten the measurement. These chambers. In the capillary regime, unbound liquid water can be found in the porous materials. Luckily, capillary regime has two distinct measures, w_f free water saturation and w_{max} maximum water content [37]. The free water saturation can be measured by immersing the samples into water at normal pressure and measuring them until equilibrium mass. We also need to supersaturate the samples to achieve 100% RH by immersing the samples into water in an evacuation vessel with the same technique as measuring its open porosity and apparent density described in MSZ EN 1936 [38].

2.3. Water vapor permeability

Water vapor permeability of materials can be measured by using the cup method according to MSZ EN ISO 12572 [39] by using a self-made chamber. As water vapor permeability could depend on the temperature and relative humidity [31], both wet and dry cup measurements were performed in the Laboratory of Building Physics, showing that permeability of fibrous materials (such as mineral wools) usually does not show dependence on the relative humidity; however, polyurethane foam or expanded polystyrene does.

2.4. Liquid transport coefficient

There is no standardized method available for measuring liquid transport coefficient of building materials in laboratory conditions. The determination according to scientific literature can be performed by using various, but time-consuming and expensive methods. Fortunately, Krus and Holm [40] presented a simple method to approximate liquid transport coefficient for suction, and I used their method to obtain liquid transport coefficient of materials.

2.5. Volumetric heat capacity

The volumetric heat capacity can be obtained by multiplying ρ density [kg/m^3] of the material with its c_p specific heat capacity at constant pressure [J/kgK]. Dry density of building materials can be measured according to MSZ EN ISO 12570 [41], while density of thermal insulation materials can be measured by using MSZ EN 1602 [42]. There is no standardized measurement method available for measuring specific heat capacity of construction materials; in the Laboratory of Building physics, we use mixing calorimetry [43] for determining the specific heat capacity of materials.

2.6. Thermal transmittance

To be able to measure U value of masonry blocks sections, I designed and built an experimental box setup shown by **Fig. 3** and **Fig. 4**. Unlike Pavlík's semi-scale device [44], which used two climate chambers, my setup consists of only one temperature chamber in which the relative humidity can be controlled by salt solutions and a valve that can be opened at certain relative humidity levels. The other side of the tested specimen contacts with the laboratory air, which temperature and humidity is controlled. The chamber contains a black painted box made of cardboard, in which the internal cold or hot humid air is circulated by using ventilators, whose speed is controllable in order to change surface resistance. In this box, temperature, relative humidity and pressure are measured by using an Ahlborn system [45]. The specimen is placed into thermal insulation frame to cover the opening. A heat flux sensor is placed on the external surface of the specimen, while the laboratory air temperature, relative humidity and pressure are also measured.

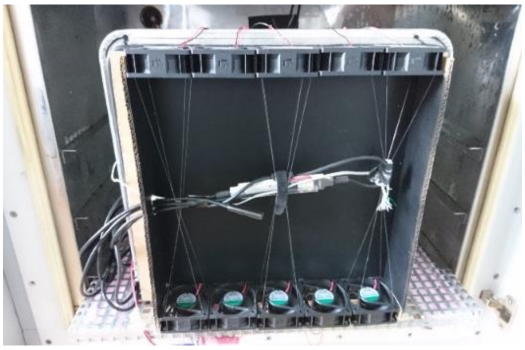

Fig. 3 Experimental box setup with adjustable speed air circulation system and measuring sensors

Fig. 4 Measuring thermal transmittance of a masonry block section

3. Numerical methods

3.1. *Hygrothermal modeling*

The schematic flow chart of the hygrothermal numerical modeling process is illustrated in **Fig. 5**. In the hygrothermal modeling, the mathematical equations are based on the conservation of energy and moisture. In the modeling process, some assumptions had to be made, i.e. the geometry is constant, there is no swelling or shrinkage due to temperature or moisture; there is no changes in the material properties due to its damage or ageing; no chemical reactions occur due to temperature or moisture; the latent heat of sorption is equal to the latent heat of condensation or evaporation; there is no hysteresis effect taken into account in the moisture storage function and its dependence on temperature is also neglected; and finally, vapor diffusion and liquid transport only depend on the relative humidity of the materials. In the simulations, two or three dimensional geometry models are used depending on the studied task. Material properties are based on the previously described laboratory measurements and standards. The initial conditions are configured to minimize the required run time of the models, so basically the average of the internal and external temperature and relative humidity were used in steady-state simulations, and preliminary results from steady-state simulations were used in dynamic simulations. Boundary conditions were set according to standards in steady-state simulations. In dynamic simulations, besides standards-based boundary conditions, some built-in boundary conditions of WUFI software (e.g. driving rain, explicit radiation balance at exterior surfaces) were also used in extended forms using different, developed formulas to describe solar radiation components.

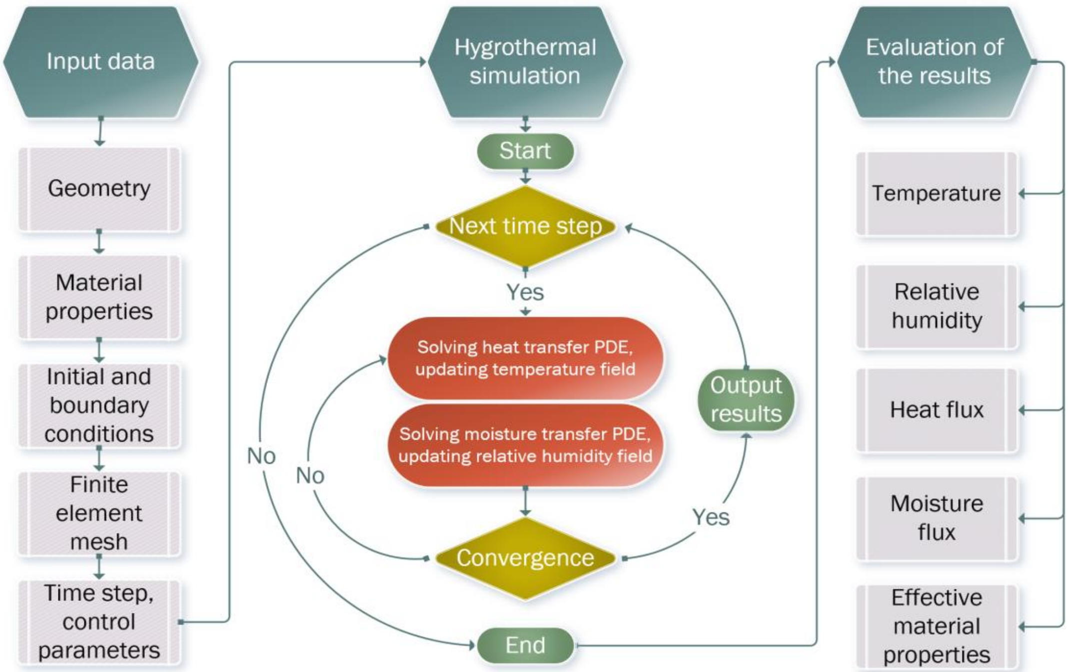

Fig. 5 Schematic flow chart of the hygrothermal modeling process

3.2. *Optimization*

COMSOL Multiphysics is capable of implementing constrained gradient-free or gradient-based optimization processes [46], which schematics are illustrated in **Fig. 6**.
There are several different gradient-free solvers available, such as Monte-Carlo method [47], which randomly chooses the design variables between the given bounds, and evaluates the results; however, with this method, the global optimum can be found only with very dense statistical sampling, resulting in long optimization time. 1st order approximate gradient methods are Nelder-Mead [48] and constrained optimization by linear approximation (COBYLA) [49]

methods. Both can take the constraints into consideration. Powell [50] presented, that Nelder-Mead algorithm can find the least value of a function incorrectly in case of convex objective function. Therefore, in the research, COBYLA was used to perform geometry optimisation of a selected thermal insulation filled masonry block.

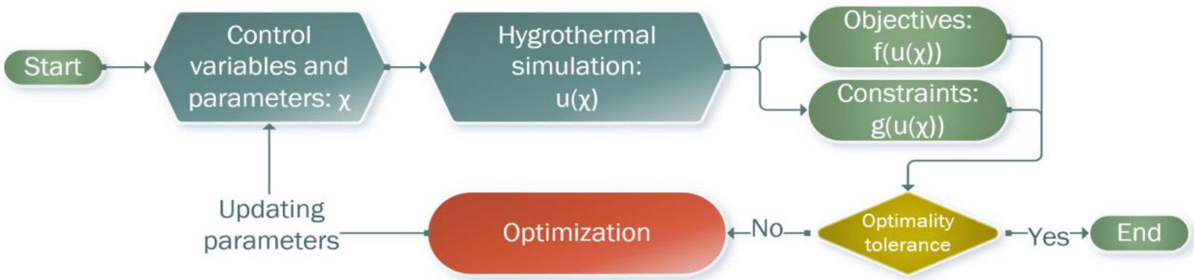

Fig. 6 Schematic flow chart of the optimization process

III. THERMAL CONDUCTIVITY OF MASONRY BLOCKS

1. Simulation methodology supported by laboratory measurements

In 2014, one of our industrial partners wanted to know the thermal conductivity of their masonry blocks. Additionally, and that caused the challenge, the manufacturer wanted to obtain thermal conductivity of a masonry block from only one prototype sample, i.e. there was no opportunity to build a sample wall and perform a full-scale model experiment. A solution based on pure numerical simulation was not acceptable, since our industrial partner required a more realistic and tangible solution based on measurements. Therefore, I had to come up with a methodology, how to obtain thermal conductivity of a masonry block based on laboratory experiments.

1.1. Methodology of the experiment

The laboratory measurement supported numerical simulation methodology can be divided into four distinct parts which follow each other.
The first step is to cut the whole prototype masonry blocks into sections, which can be measured in the Laboratory of Building Physics. From the selected masonry blocks, we need to cut at least three representative sections, with the thickness under 10 cm.
The second step is to measure the thermal conductivity of the samples. Since the selected masonry blocks have a height and width of around 25 cm, the cut sections have to be placed into a thermal insulation frame, since the thermal conductivity measuring device accepts 30 cm x 30 cm samples.
FEM based thermal simulation of the masonry block sections is the third step in the process. After measuring the geometry of the masonry block and its hollows by using calibrated digital caliper gauge, a 3D CAD model is prepared and the numerical simulations as well as the parametric calibration process within the simulations are performed by using the capabilities of Ansys Workbench [51], and its mechanical module for steady-state thermal simulations. At first run, the sections were modeled with initial material properties. During the calibration process, two material properties had to be optimized to obtain the same thermal conductivity from the simulation as measured. It facilitates the process if the range of the thermal conductivity of materials is known by individual measurements. Through the simulation and calibration process, the material properties are iterated until the simulated thermal conductivity of the block section differs only maximum 1.0 % compared to measured results at the same iteration step for all three sections.
After obtaining the calibrated thermal conductivity of materials, the simulation process of whole masonry block and a tongue-groove connected model is performed using these properties as the final step. The whole process of laboratory measurement supported numerical simulation

modeling of masonry blocks to obtain its thermal conductivities is summarized in **Fig. 7**. In the dissertation, I presented the method in use on three different hollow or filled masonry blocks and obtained their thermal conductivity with good accuracy.

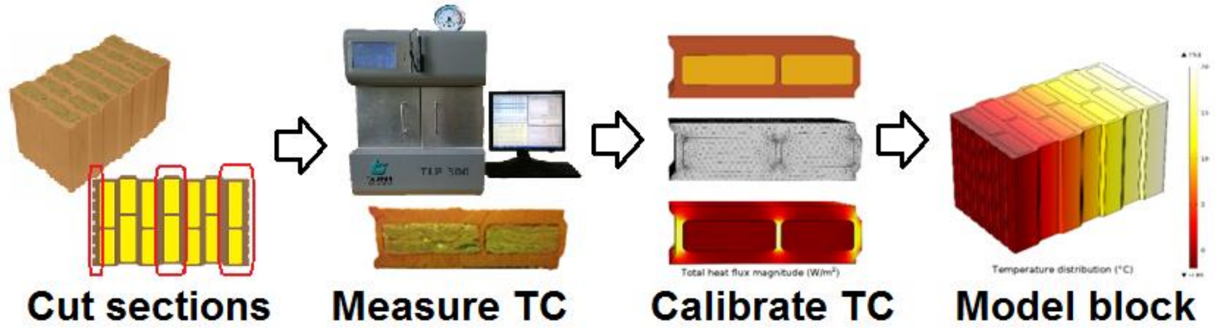

Fig. 7 Process of the laboratory measurement supported simulation modeling

1.2. Presentation of the method with 3 selected masonry blocks

One of the presented prototype masonry blocks is called “S38” because of its 38 cm thickness and has only small rectangular hollows. The second prototype block is called “K44-EXP” and its triangular and rectangular hollows are filled with expanded perlite. The third block is called “T44-MW” and it was marketed in Hungary at the time when the study was performed. Both latter masonry blocks were 44 cm thick. The blocks were cut into three sections and the sections were measured. The results are summarized in **Table 1**.

Table 1 Thermal conductivity of measured and simulated sections of T44 with MW filler

Sample	**T44-MW1**	**T44-MW2**	**T44-MW3**
Thickness, d [mm]	19.29	78.35	79.24
Density, ρ [kg/m^3]	1598.1	904.9	925.9
Thermal conductivity, $\lambda_{10,lab}$ [W/mK]	0.363	0.100	0.117
Thermal conductivity, $\lambda_{10,sim}$ [W/mK]	0.36	0.1003	0.1171
Difference [%]	0.83	0.26	0.04

Using the presented simulation method supported by laboratory measurements, the thermal conductivities of the masonry blocks were obtained. The results are summarized in **Table 2**.

Table 2 Thermal conductivity of measured and simulated sections of T44 with MW filler

Sample	**T44-MW1**	**T44-MW2**	**T44-MW3**
Thickness, d [mm]	19.29	78.35	79.24
Density, ρ [kg/m^3]	1598.1	904.9	925.9
Thermal conductivity, $\lambda_{10,lab}$ [W/mK]	0.363	0.100	0.117
Thermal conductivity, $\lambda_{10,sim}$ [W/mK]	0.36	0.1003	0.1171
Difference [%]	0.83	0.26	0.04

In terms of results, it can be stated that there is no significant difference between the equivalent thermal conductivity unfilled and EXP filled masonry blocks. These two tested blocks have different geometry, however their $\lambda_{block,sim}$ results are very close to each other. It seems, that expanded perlite filled blocks in reality cannot brought the expected performance increase reported by [52], [53]. In case of T44-MW, our industrial partner had a measured thermal conductivity value of their MW filled blocks which was 0.084 W/mK, therefore the difference between large-scale measurement and my approach was only 3.5 %. This difference can occur because of the different conditions; dried samples has better values and my process was performed under laboratory conditions. This difference considered as sufficient accuracy to use this new method to test prototype masonry blocks for our industrial partner. The costs and time of investigation in case of the new method is significantly less than performing a large-scale test, and only one prototype masonry block is needed.

1.3. Validation the method by a measured masonry block section

With the setup shown previously by **Fig. 3** and **Fig. 4**, a validation measurement was constructed to test the thermal conductivity of selected masonry block section shown in **Fig. 8**. The surface temperature from the side of the laboratory, during the measurement and after the removal of the heat flux plate was recorded by using a Testo 885-2 thermal imager [54]. Before the measuring session, the sample placed to its position and preconditioned for two weeks. To test the moisture equilibrium to determine whether the measurement period could start, a Protimeter MMS2 [55] was used. The measurement period lasted for a week. The calculated thermal conductivity based on the measurements was shown in **Fig. 9**. For the final averaged value, 72 h of measured data were used. The thermal transmittance of the measured area of T44-MW2 section was U = 0.8914 W/m^{2}K, from which the thermal conductivity is $\lambda_{hf,lab}$ = 0.0867 W/mK. **Fig. 10** shows surface temperatures, giving θ_{AV1}= 22.6 °C on the surface facing to the lab, while the average surface temperature of the chamber side of the block was based on the measurements performed by the NiCr-Ni thermowire and it resulted in $\theta_{s,chamber}$ = 6.64 °C. The measured $\lambda_{hf,lab}$ was lower (0.0866 W/mK), than the value measured by Taurus TLP 300 DTX (0.1 W/mK), because the heat flux sensor was positioned differently to try to measure mostly the core of an insulation filled cavity and reduce the effect of the internal fired clay wall, while during the guarded hot plate measurements, its sensors were placed to the center of the surface. Therefore, to validate the measurements by guarded hot plate, numerical simulation was needed.

Fig. 8 T44-MW2 section

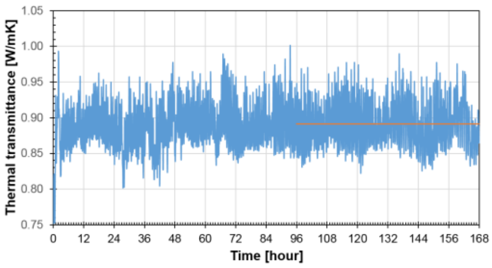

Fig. 9 Measured $\lambda_{hf,lab}$ of T44-MW2 section

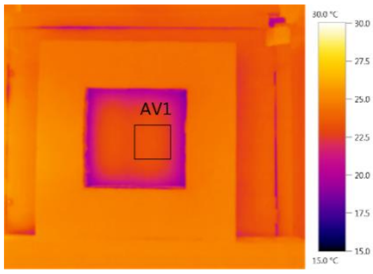

Fig. 10 Thermal image of setup after measurement

The 3D steady-state numerical simulation to reproduce the measured result was conducted by using COMSOL Multiphysics, i.e. a hygrothermal model was implemented to perform the validation. The sensor was also modeled and placed onto the model to locate the area where heat flux needs to be retrieved. The model geometry is shown in **Fig. 11**. The simulated surface temperature distribution viewed from the lab side is shown in **Fig. 12**. This figure can be compared to **Fig. 10** and shows good agreement with the temperature distribution measured using a thermal imager. **Fig. 13**. illustrates the U value if it is calculated in each point of the surface from the surface heat flux data and the internal and external temperature differences.

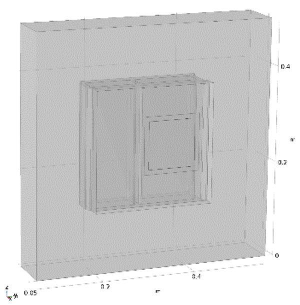

Fig. 11 Geometry model of the T44-MW2 section in its stocks

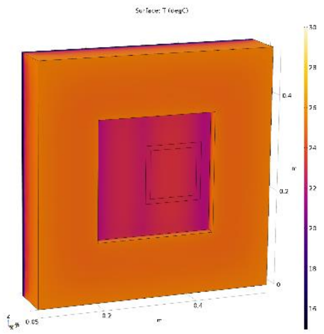

Fig. 12 Simulated surface temperature distribution

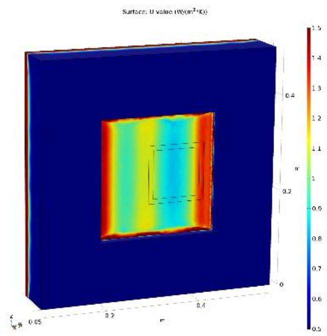

Fig. 13 Simulated distribution of the U value at surface

The simulated equivalent U value of the same surface of the tested block was U = 0.9096 W/m^{2}K, and thermal conductivity of the same surface of the block was $\lambda_{hf,sim}$ = 0.08898 W/mK. The simulated thermal transmittance is slightly larger, but differed only by 2%. The equivalent thermal conductivity showed 2.5% relative error from the measured value, which I considered acceptable, because it is smaller than the error from guarded hot plate measurements, without any calibration of the material properties. The surface temperature of the chamber side of the block was 6.57 °C and the lab side was 22.9 °C. These also show good agreement with the measurements.

2. Thermal conductivity considering different fillers

To get deeper understanding on the temperature conductivity of hollow and filled modern masonry blocks, a numerical simulation study was made considering the same individual blocks and their tongue-and-groove connected versions. In this study, the calibration procedure was not used, therefore the geometry and materials remained in their individually measured conditions. For achieving the best possible results, material properties were used with their dry measured values instead of laboratory conditioned properties. Knowing the results shown in **Fig. 14**, it can be stated that in every case, the filled building blocks have lower thermal conductivities and large air voids in building blocks are the worst in terms of thermal performance and must be avoided. Comparing individual block and tongue-and-groove connected block's values, in almost every case the individual blocks had smaller thermal conductivities (except the building block with large rectangular hollows. Blocks containing aerogel has the lowest equivalent thermal conductivities as expected, and the values are almost the same for every blocks. The internal structure of blocks becomes more important, when the fillings have higher thermal conductivities. Nowadays, most of the blocks with small hollows have well-optimised structures. Using expanded perlite for filling is worth only for large hollows since in smaller rhombus, triangular or rectangular hollows, this material has almost the same values as empty. PUR foam can significantly increase the insulation capabilities of a building block as well and it has better results than mineral wool fillings; however, its hygrothermal performance is a question needed to be answered. The results also show that in case of modern filled masonry blocks, large rectangular filled hollows have the best performance.

3. Parametric study on material properties

A parametric numerical study was made using the same simulation technique described in the previous section. In the dissertation, I included the parametric study of the T44 material geometry, because this was the best performing filled modern masonry block and also this type is the most common. The range for the thermal conductivity of the fired clay was set to between λ_{clay} = 0.2 W/mK and λ_{clay}= 0.8 W/mK, in between the steps changed by 0.025 W/mK. This resulted in 25 steps. This range was selected, because in MSZ EN 1745 [56] thermal conductivity of fired clay is tabulated according to its net dry density, and these are the lowest and highest values, the former belongs to 1000 kg/m^3, the latter one to 2400 kg/m^3. However, it is worth to note that due to mechanical aspects, density of the fired clay used for producing hollow or filled masonry blocks in Hungary is usually above 1400 kg/m^3 and thermal conductivity is above 0.3 W/mK. This limitation of the density is also needed to provide the necessary mechanical properties. The range of the thermal conductivity of the filler material was set to between λ_{filler} = 0.01 W/mK and λ_{filler} = 0.07 W/mK, in between the steps changed by 0.0025 W/mK. This range was selected, to model the possible solid or loose filled materials available nowadays from aerogel to expanded perlite. The results of numerical simulations were indicated in a contour map, which could be handled and understood easily. Data contouring process was performed by using Surfer [57]. Firstly, an interpolated grid was made by using

Kriging interpolation, but it turned out, that in this case Kriging interpolation gave results with significant errors at border zones of the map. Since it is not possible to significantly widen the range of simulated results, since we cannot implement zero or negative thermal conductivity for filler materials to run numerical simulations. Therefore, a different approach, radial basis function based interpolation technique was used for the creation of the final contour map shown by **Fig. 15**. An approximate formula for calculating λ_{T44} thermal conductivity of a 44 cm thick thermal insulation filled masonry block using λ_{clay} thermal conductivity of fired clay and λ_{filler} thermal conductivity of the filler was also created. I concluded that, the approximated λ_{T44} values obtained by using my formula compared to the results obtained by numerical simulations were under ± 1 % relative error. The formula is shown by Eq. (1):

$$\lambda_{T44} = -5.2913 \cdot \lambda_{clay}{}^2 \cdot \lambda_{filler}{}^2 - 0.169 \cdot \lambda_{clay}{}^2 \cdot \lambda_{filler} + 8.2341 \cdot \lambda_{clay} \cdot \lambda_{filler}{}^2 + 0.2312 \cdot \lambda_{clay} \cdot \lambda_{filler} + 0.12 \cdot \lambda_{clay} - 4.2216 \cdot \lambda_{filler}{}^2 + 1.2963 \cdot \lambda_{filler} \quad (1)$$

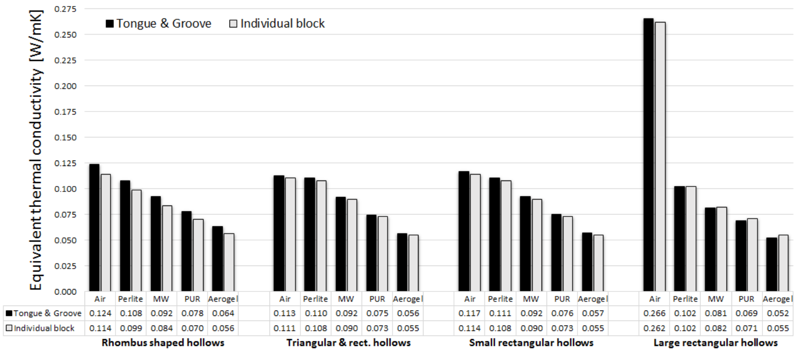

Fig. 14 Equivalent thermal conductivity of four different masonry blocks with different fillers

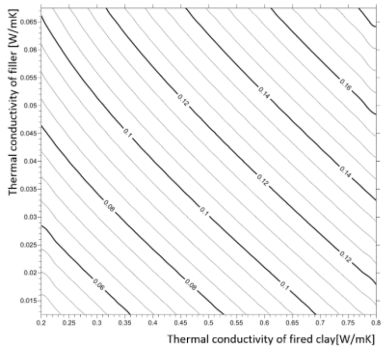

Fig. 15 Contour map of thermal conductivity of the T44 block

Thesis 1: Analysis of thermal conductivity of masonry blocks
Related publications: [NB1], [NB2], [NB3], [NB4]

I performed analysis in three approaches on differently shaped hollow or filled masonry blocks filled to determine their equivalent thermal conductivity.

1.1 I have developed a numerical thermal modeling procedure supported by laboratory measurements for testing the equivalent thermal conductivity of prototype masonry blocks. I validated the method using different measurement techniques and hygrothermal numerical simulations. I found, that using the new method, the equivalent thermal conductivity of a hollow or filled masonry block can be determined accurately.

1.2 Based on numerical simulations supported by laboratory measurements and additional simulation studies, I determined the equivalent thermal conductivity of four differently shaped masonry block filled with five different materials. I showed, that filling expanded perlite into masonry blocks which have small and narrow cavities does not cause significant improvement in thermal conductivity and should be avoided.

1.3. Based on a systematic parametric numerical simulation study, I determined the values and limitations of the effective thermal conductivity of the most commonly used 44 cm thick thermal insulation filled masonry block. I visualized the results on a contour map and developed an approximate function to obtain the thermal conductivity of the filled masonry block depending on the thermal conductivity of its fired clay and thermal insulation filler material.

IV. HYGROTHERMAL PERFORMANCE OF MODERN MASONRY CONSTRUCTIONS

1. Input data

In this study, wall constructions are handled with their complex geometries, which contain their inner structures as well. This detailed modeling makes it possible to analyze the building constructions in their depths and get deeper understanding about their hygrothermal behavior. Detailed 2D geometry models of the evaluated building constructions, horizontal wall section and wall corner section, are shown in **Fig. 16** and **Fig. 17**.

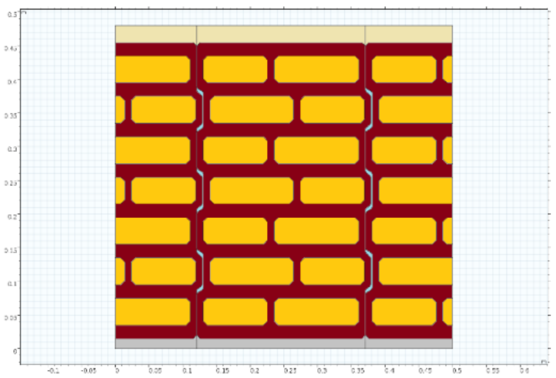

Fig. 16 Model of the masonry wall

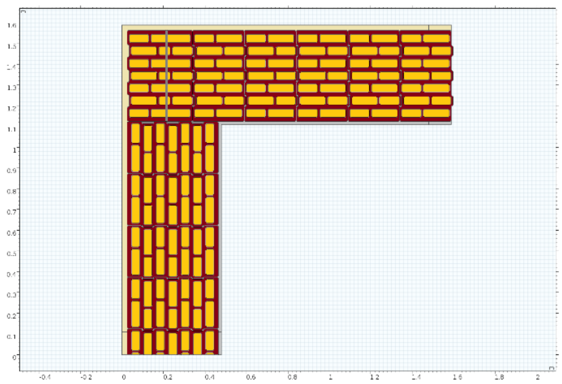

Fig. 17 Model of masonry wall corner joint

Material properties of the thermal insulations, fired clay (FC), internal plaster (IP) and external plaster (EP) are listed in **Table 3**, and were measured in laboratory, such as $\lambda_{10,dry}$ thermal conductivity [W/mK] with addition of f_T temperature and f_ψ moisture dependent conversion factors from MSZ EN ISO 10456 [35], ρc_p volumetric heat capacity [J/m^{3}K], $\mu_{dry/wet}$ water vapor resistance factor [1] and $D_{w,s}$ liquid transport coefficients of suction at moisture content of 80% relative humidity [m^2/s].

Table 3 Hygrothermal material properties

Material	AG	PUR	MW	EPS	EXP	FC	IP	EP
Thermal conductivity, $\lambda_{10,dry}$ [W/mK]	0.012	0.024	0.031	0.037	0.05	0.35	0.4	0.09
Temperature conversion factor, f_T [1/K]	0.0015	0.0055	0.0045	0.0035	0.0035	0.001	0.001	0.001
Moisture conversion factor, f_ψ [m^3/m^3]	3	6	4	4	3	10	3	8
Volumetric heat capacity, ρc_p [J/m^{3}K]	120	49	75	22.5	81	1280	722.5	540
Water vapor resistance factor, $\mu_{dry/wet}$ [1]	4.5	80/70	1.3	70/30	2	15/10	8.1	8.3
Liquid transport coefficient, $D_{w,s,80\%}$ [m^2/s]	$1.7\cdot10^{-14}$	$5.5\cdot10^{-21}$	$4.6\cdot10^{-13}$	$2.4\cdot10^{-20}$	$1.0\cdot10^{-13}$	$2.3\cdot10^{-9}$	$3.0\cdot10^{-9}$	$1.3\cdot10^{-13}$

The moisture storage curves of the materials were also determined as shown separately for materials with different ranges of moisture content by **Fig. 18**, **Fig. 19**, and **Fig. 20**.

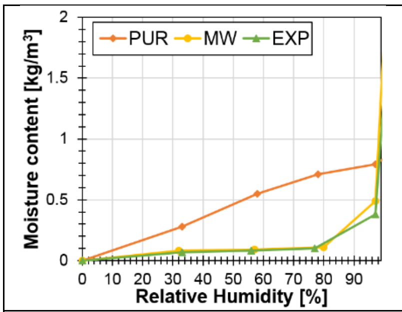

Fig. 18 Moisture storage function of PUR, MW and EXP

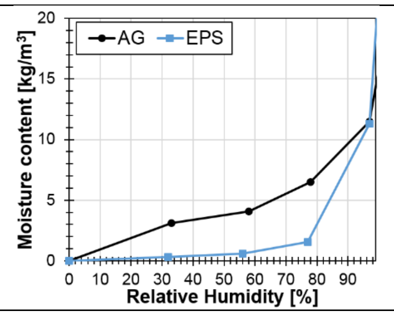

Fig. 19 Moisture storage function of AG and EPS

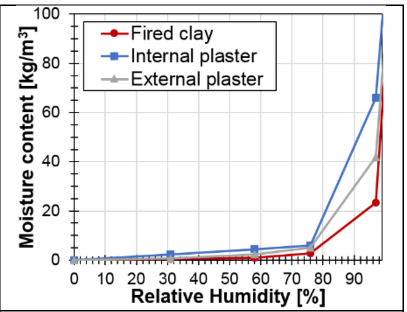

Fig. 20 Moisture storage function of FC, IP and EP

The boundary conditions used in the study presented in this chapter are based on weather files with hourly resolution of Budapest (Hungary), Espoo (Finland) and Lisbon (Portugal) generated by using Meteonorm [58]. The internal temperature and relative humidity is calculated on the basis of external temperatures. Hourly external temperature and relative humidity (RH) are shown by **Fig. 21** and **Fig. 22**. Internal temperature and RH values were created according to the standard [59] based on the external temperatures. onthly averaged values of Budapest summarized in **Table 7** was used in steady-state cases.

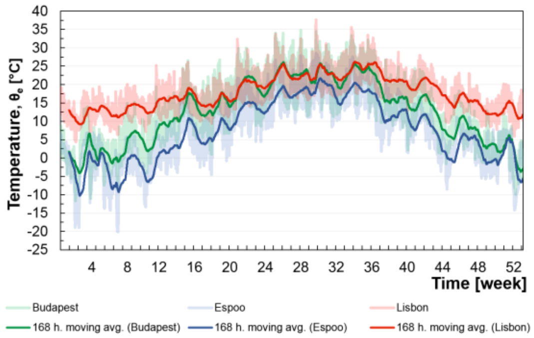

Fig. 21 External temperature

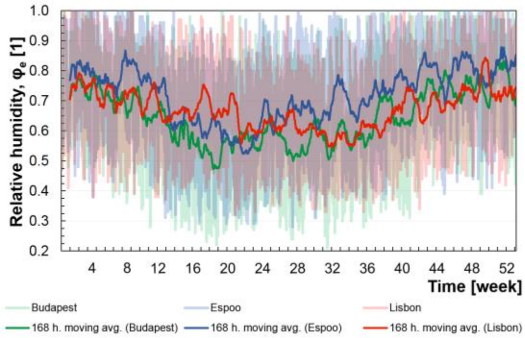

Fig. 22 External relative humidity

Table 4 Monthly average temperature and relative humidity data of Budapest, Hungary

Month	I.	II.	III.	IV.	V.	VI.	VII.	VIII.	IX.	X.	XI.	XII.
Temperature, θ_e [°C]	0.9	2.8	7.0	13.3	18.4	21.4	23.1	22.8	17.4	12.5	7.2	1.7
Relative humidity, φ_e [1]	0.73	0.68	0.61	0.52	0.53	0.54	0.54	0.54	0.62	0.69	0.73	0.74
Wind speed, v [m/s]	1.4	1.7	2.0	1.7	1.7	1.6	1.7	1.4	1.4	1.2	1.6	1.2
Temperature, θ_i [°C]	20.0	20.0	20.0	21.7	24.2	25.0	25.0	25.0	23.7	21.3	20.0	20.0
Relative humidity, φ_i [1]	0.41	0.43	0.47	0.53	0.58	0.60	0.60	0.60	0.57	0.53	0.47	0.42

When dynamic simulations were performed with hourly time steps and the effect of orientation and climate of the structures were also evaluated, boundary fluxes based on explicit radiation balance and driving rain were also considered based on the climate dependent weather files. Excerpts of the boundary conditions used shown by **Fig. 23** - **Fig. 28**.

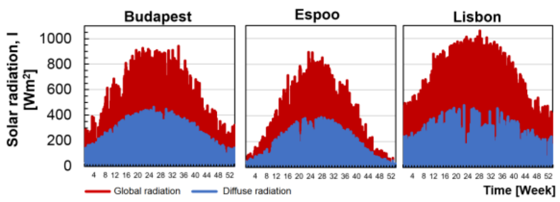

Fig. 23 Global horizontal and diffuse solar radiations

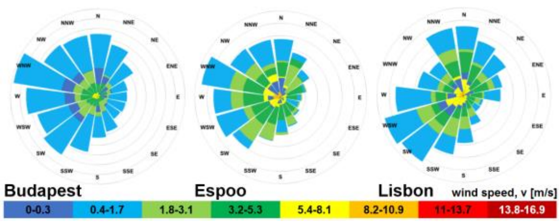

Fig. 24 Wind roses

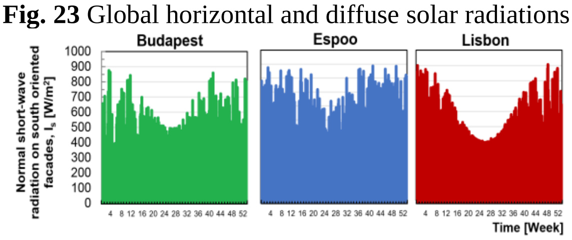

Fig. 25 Normal short-wave radiations on south façades

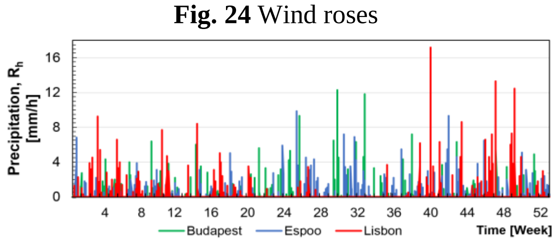

Fig. 26 Precipitations on horizontal surfaces

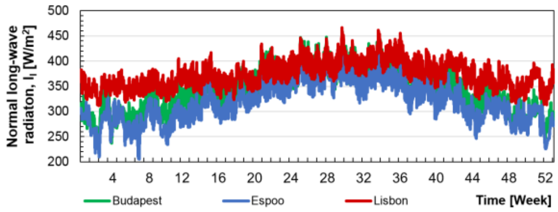

Fig. 27 Normal long-wave radiations

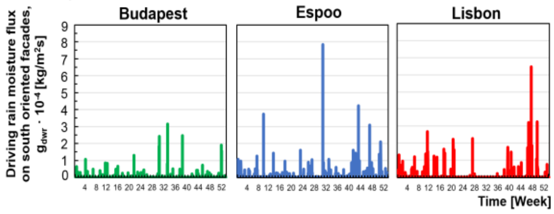

Fig. 28 Driving rain moisture fluxes on south façades

2. Thermal transmittance

2.1. Steady-state and dynamic U value of walls

Fig. 29 shows the results of the steady-state numerical simulations. Additionally, besides the conjugated heat and moisture transfer simulations, three different set of simulations were performed with different settings. The first case was a thermal simulation, where only heat transfer was considered with temperature dependent thermal conductivities. In the second case, I neglected the heat fluxes coming from evaporation fluxes and in the third case, temperature, RH and wind-dependent, variable boundary conditions were used instead of the simplified values of standards [59], [60]. It is observable in **Fig. 30**, which presents averaged values over the heating season (November-March), that there is difference between thermal and hygrothermal simulations, however only slight differences are visible if evaporation fluxes are neglected and variable boundary conditions do not show any differences. Additionally, in the dissertation, ψ values of wall corners were also presented and evaluated.

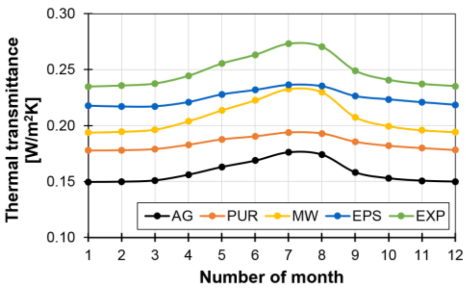

Fig. 29 Monthly steady-state U values based on HAM simulations

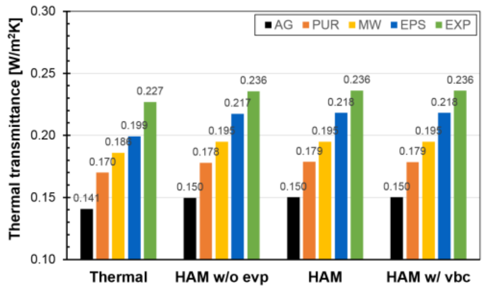

Fig. 30 Heating season averaged U values of thermal, HAM w/o evp, HAM and HAM w/vbc simulations

Environment dependent U values were examined using time dependent simulations with climate dependent boundary conditions. In dynamic simulations, effective hourly based U value shows the amount of heat loss or heat gain per internal unit surface according to the temperature difference. This value also shows the direction of heat flow on the internal surface, positive value means heat loss and negative is connected to heat gain. The monthly averaged dynamic U values are presented in **Fig. 31** for all four different façade orientations in Budapest.

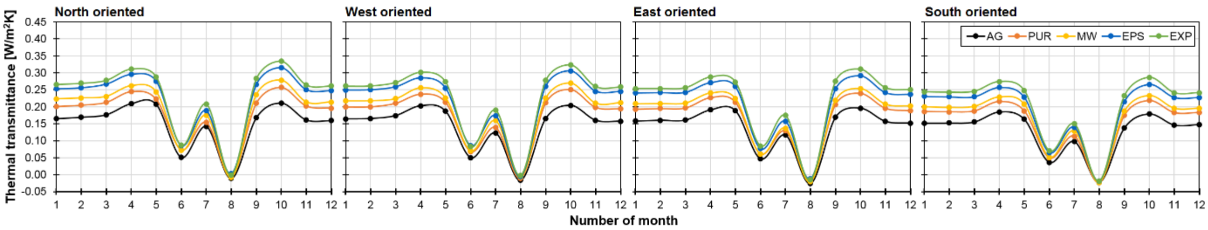

Fig. 31 Dynamic U values of walls made of 44 cm thick insulation filled blocks depending on the orientation

In the months of the heating season, the difference between dynamic and steady-state results are positive, which means that dynamic simulations gave higher U values. However, in summer, differences show very big negative differences. If we average the values of the year, the dynamic U value results are smaller than steady-state results shown by **Fig. 32**. (There is only one exception: in case of north oriented EPS filled wall it is 1.4% higher). However, if we analyze the results only for the heating season shown by **Fig. 33**, it is clearly visible, that dynamic simulated results are always higher than steady-state. South oriented walls show the differences, between 0.5% and 5.0%. Therefore, it seems that it can be acceptable to use steady-state simulation instead of dynamic in this case. However, differently oriented façades show greater differences, a dynamic simulated average U value in the heating season north facing wall can differ up to 16.9% compared to steady-state. The differences are big enough to show the necessity of handling the U values of the building envelope separated by their orientations. This leads to the conclusion that thermal performance of wall constructions made of 44 cm thick thermal insulation filled masonry blocks should be calculated by using orientation-dependent dynamic hygrothermal simulations.

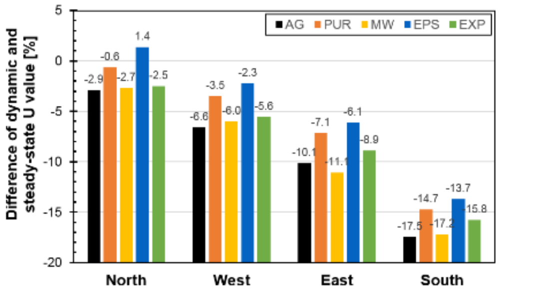

Fig. 32 Yearly averaged U value differences dynamic HAM and steady-state HAM simulations

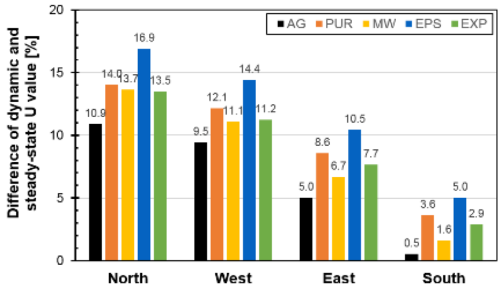

Fig. 33 Heating season averaged U value differences of dynamic HAM and steady-state HAM simulations

2.2. Climate-dependent U value of walls

The same numerical simulation process was performed on the oriented wall models by using Espoo and Lisbon climate data as the basis of boundary conditions. The monthly averaged U value results are summarized in **Fig. 34** for Espoo and **Fig. 35** for Lisbon. The monthly variation of results compared to Budapest are different in both cases. The transitional periods are in different position, and in Espoo, the heating season seems at least two months longer than in Budapest, while in Lisbon, it is shorter. In both climates, there are no negative values in the summer, however, in Espoo, similar drop in the U values are observable.

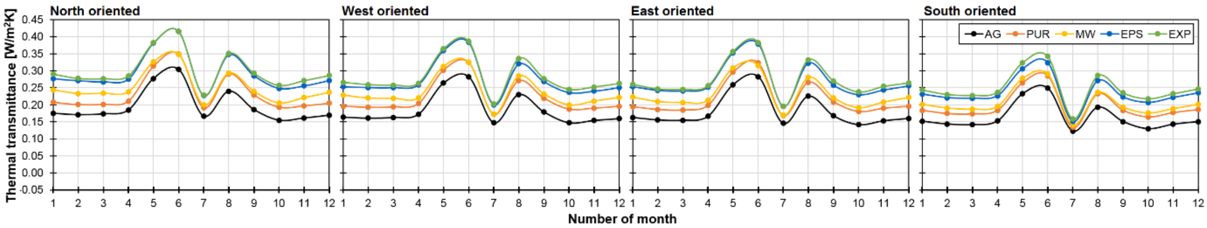

Fig. 34 Dynamic simulated and monthly averaged U values of oriented walls considering Espoo climate

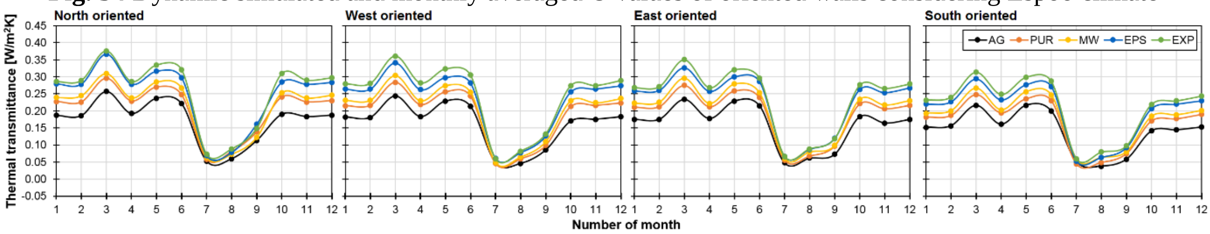

Fig. 35 Dynamic simulated and monthly averaged U values of oriented walls considering Lisbon climate

In **Fig. 36** and **Fig. 37**, the differences between the average values of the heating season are summarized. In these cases, heating season considered also between November and March for the sake of comparability. These two figures show similarity in the heating season in Budapest and Espoo, since the differences remain under 5.6% and in some cases, Budapest U values are higher by up to 3.3%. On the other hand, U values in Lisbon differ by from 3.7% up to 20.1%. However, there is only small differences between the values in the heating season in Espoo and Budapest, but there are considerably large differences occur between Lisbon and Budapest. Therefore, in technical datasheets, different U values should be given in different climates for the same wall made of 44 cm thick thermal insulation filled masonry blocks.

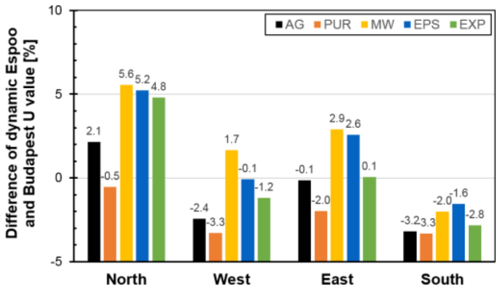

Fig. 36 Heating season U value differences between Espoo and Budapest

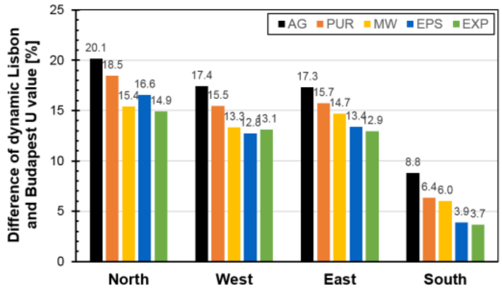

Fig. 37 Heating season U value differences between Lisbon and Budapest

Thesis 2: Thermal transmittance of insulation filled masonry blocks
Related publications: [NB7], [NB9], [NB11]

I performed steady-state thermal and hygrothermal simulations of walls and wall corner joints, and environment-dependent dynamic hygrothermal simulations of walls made of 44 cm thick masonry blocks filled with 5 different thermal insulations in three different climates (Budapest, Espoo, Lisbon) to analyze their thermal transmittances.

2.1 I showed that although yearly averaged U values obtained by dynamic simulations are lower than steady-state simulated results, heating season averaged U values show 0.5% - 16.9% positive difference depending on the filler material and the orientation of the wall. Therefore, thermal performance of wall constructions made of 44 cm thick thermal insulation filled masonry blocks should be calculated by using orientation-dependent dynamic hygrothermal simulations.

2.2 I have showed that there are only small differences between the U values in the heating season comparing Espoo and Budapest, but there are considerably large differences between Lisbon and Budapest. Therefore, in technical datasheets, different U values should be given in different climates for the same wall made of 44 cm thick thermal insulation filled masonry blocks.

3. Moisture transmittance

3.1. Comparison of thermal and moisture transmittances

I have recently raised the need for a method that provide easily comparable results to evaluate the moisture transport behavior of complex building elements and construction joints, besides analyzing their simulated moisture content or relative humidity, which is now the standard methodology in these evaluations; however, these analyses are only available when we perform dynamic simulations, which can be demanding to handle due to the increased need of computational efforts and necessary material properties. The method I came up with to analyze the moisture performance is somewhat similar to the method we use to deal with thermal problems and works by using steady-state approach. I introduced moisture transmittance and linear moisture transmittance of building constructions. I present my approach by comparing thermal and moisture transmittances of two wall corner joints made of EPS or MW filled masonry blocks. During this example, I also showed how the equivalent water vapor diffusion resistance of the masonry constructions developed, since in the available domestic technical datasheets of masonry blocks filled with either EPS or MW, it is given as 5/10, according to MSZ EN 1745 [56]. This value does not seem appropriate at first glance. If it is correct, we should obtain the same moisture transmittance and linear moisture transmittance values in this study for both wall and wall corner joints.

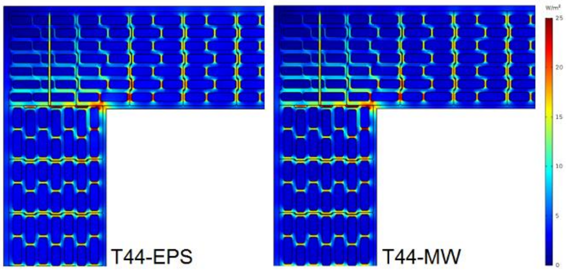

Fig. 38 Heat flux magnitudes in wall corner joints made of EPS and MW filled masonry blocks

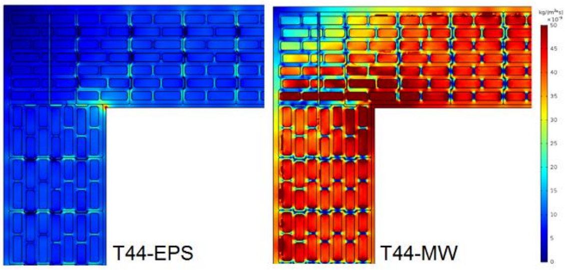

Fig. 39 Moisture flux magnitudes in wall corner joints made of EPS and MW filled masonry blocks

After performing the simulations, heat flux magnitudes in the horizontal cross-sections of the investigated constructions are visualized in **Fig. 38**, while the moisture flux magnitudes are shown in **Fig. 39**. It is clearly visible, that while heat fluxes do not differ much, moisture fluxes show great differences. The results are summarized in **Table 5**.

Table 5 Results of the comparative analysis of thermal and moisture transmittances of T44-EPS and T44-MW

Case	$U_{wall,THERM}$ [W/m²K]	$U_{wall,HAM}$ [W/m²K]	$\psi_{corner,THERM}$ [W/mK]	$\psi_{corner,HAM}$ [W/mK]	$M_{wall} \cdot 10^{-12}$ [kg/m²·s·Pa]	μ_{eqv} [1]	$\nu_{corner} \cdot 10^{-12}$ [kg/m·s·Pa]
T44-EPS	0.20	0.22	0.090	0.095	5.7	33.4	1.4
T44-MW	0.18	0.19	0.088	0.091	22.8	8.5	5.8

Analyzing the results shown by **Table 5**, we can see that while thermal and hygrothermal U and ψ values does not show great differences, M values (moisture transmittances) and ν values (linear moisture transmittances) show significant differences. It can be seen that the masonry wall built of mineral wool filled blocks can pass about 3.88 times more moisture under unit time and pressure than EPS filled ones, and in a wall corner joint, the corner constructed of MW filled blocks also let through more than 3 times as much moisutre, as EPS filled ones.

3.2. Effective water vapor diffusion resistance factor of walls and wall corners

During the previous example, on the basis of this results shown by **Table 5**, we can see that in case of MW filler, the μ_{eqv} equivalent water vapor diffusion resistance is between 5/10, therefore it seems that it can be used in simplified calculations. However, in the case of EPS filled blocks, the equivalent $\mu_{T44\text{-}EPS}$ is more than 3 times the wet cup value. Therefore in the case of this filler, using 5/10 as an assumed value leads to calculation errors. To further demonstrate the possible differences, effective water vapor diffusion resistance factor of walls and wall corner joints were also evaluated to both five different fillers used previously, and the results are summarized in **Fig. 40** and **Fig. 41**. It is visible that walls and corners made of PUR and EPS filled blocks in the heating season have much higher resistance against vapor, than AG, MW or EXP masonry. It can be stated, if the vapor permeability of the filler material is higher than the fired clay shell, then using the values of fired clay could be acceptable. However, if the permeability of the filler is lower, therefore resistance is higher, using the values of fired clay as substitution leads to miscalculations in the heating season.

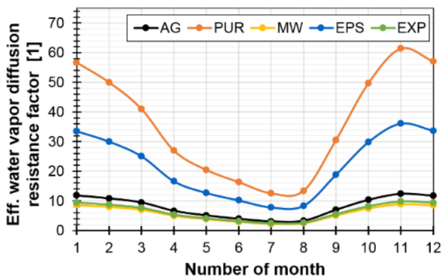

Fig. 40 Effective water vapor diffusion resistance factor of wall constructions

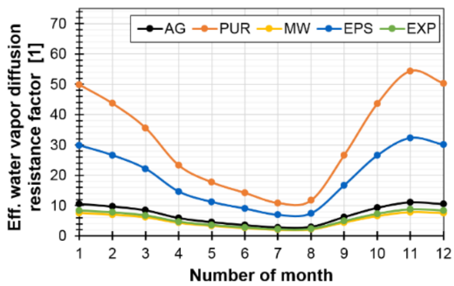

Fig. 41 Effective water vapor diffusion resistance factor of wall corner joints

3.3. Linear moisture transmittance of moisture bridges

According to my approach, it is not only possible to analyze thermal bridges of constructions, but additionally the effect of moisture bridges, as I demonstrated earlier. Moisture bridges are those part of the structure, where additional moisture loss occurs due to multidimensional moisture (both diffusion and capillary) fluxes. The question is whether it makes sense to separate moisture bridges from thermal (or hygrothermal) bridges, and analyze moisture bridges separately. In the previously presented comparative analysis between T44-EPS and T44-MW used January monthly boundary conditions only. To further demonstrate the usability of analyzing linear moisture transmittances, I simulated the wall and wall corner joints for each month and considered five different fillers as well. I made the calculations using thermal simulations, the results of that study is shown in **Fig. 42**. Evaluating the linear moisture transmittances shown in **Fig. 43**, and comparing the results to linear thermal transmittances, it is visible that while ψ values are between 0.08 and 0.1 W/mK and do not show great differences. It can be observed that, in the case of linear moisture transmittances, its trends and differences are completely different than what obtained by analyzing linear thermal transmittances. ν values show differences up to 5.2 times in January between the ν values of PUR and MW filled constructions, and there is 3.5 times difference in July.

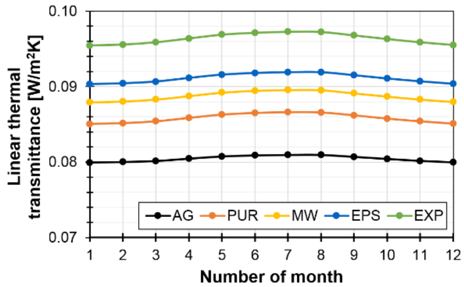

Fig. 42 Linear thermal transmittance of wall corner joints based on thermal simulations

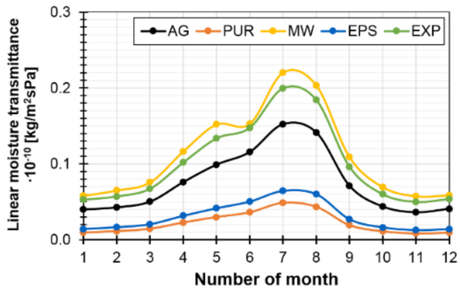

Fig. 43 Linear moisture transmittance of wall corner joints based on HAM simulations

Thesis 3: Moisture transmittance of insulation filled masonry blocks
Related publications: [NB6], [NB9], [NB11]

I introduced a new approach to evaluate the moisture performance of building constructions by using stead-state hygrothermal simulations by calculating moisture transmittance and linear moisture transmittance and the effective water vapor diffusion resistance factor.

3.1 I showed that, while the heat transfer was quite similar and showed only 5.5% to 10% difference between walls made of mineral wool and expanded polystyrene filled masonry blocks, moisture transmittance was more than 300% higher in the case of mineral wool filled blocks comparing to expanded polystyrene filled ones.

3.2 I determined the monthly averaged effective water vapor diffusion resistance factor of walls and wall corners made of five differently filled 44 cm thick masonry blocks. I have showed that if the vapor permeability of the filler material is higher than the fired clay shell, then using the values of fired clay could be acceptable, how the current standard requires it. However, if the permeability of the filler is lower, using the values of fired clay as substitution leads to significant miscalculations in the heating season.

3.3 I defined the concept of moisture bridges, and its measuring by linear moisture transmittance. I have showed that, in case of wall corner joints made of 44 cm thick thermal insulation filled masonry blocks, moisture bridges behave differently than thermal bridges.

4. Durability

In durability analysis, vapor condensation potential and possible freeze-thaw cycles in the outermost thermal insulation layer within a filled, 44 cm thick masonry block were investigated under Budapest climate conditions. Firstly, a MW filled block was tested using different methods and their results were compared to select the method that is useable to perform the task. The methods used were 1D calculation according to MSZ EN ISO 13788, 2D and 3D steady-state hygrothermal simulation and orientation-dependent 2D dynamic hygrothermal simulation. Excerpts of this study is shown by **Fig. 44**, **Fig. 45**, **Fig. 46**, **Fig. 47, Fig. 48** and **Fig. 49**. Thereafter, all five fillers were included using the selected orientation-dependent dynamic hygrothermal approach. I have analyzed how many freeze-thaw cycles are expected in the outermost layer in case of different thermal insulations during their service life of 50 years.

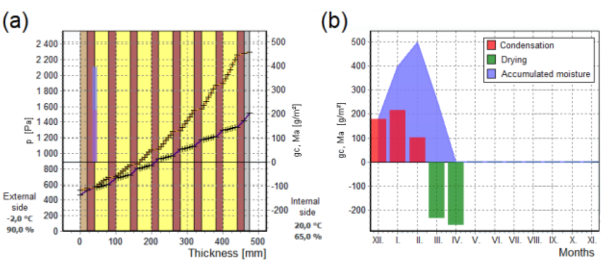

Fig. 44 1D calculation according to MSZ EN ISO 13788 showing: (a) saturation and partial vapour pressure in January (design) and (b) monthly based moisture accumulation in outermost MW layer

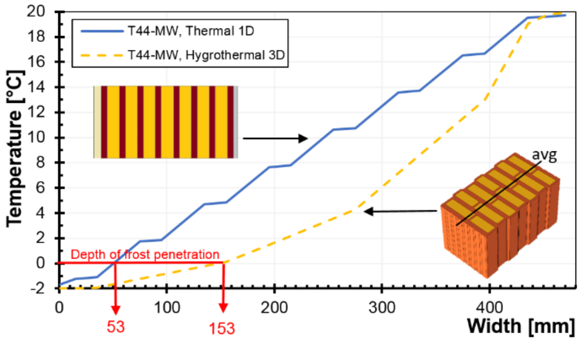

Fig. 45 Comparison of 1D thermal approach and 3D hygrothermal approach on the temperature distribution within T44-MW filled masonry block showing depth of frost penetration

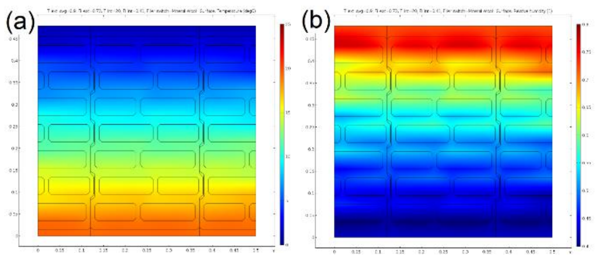

Fig. 46 2D temperature (a) and relative humidity (b) distribution based on steady-state HAM simulation considering BC based on January monthly averages

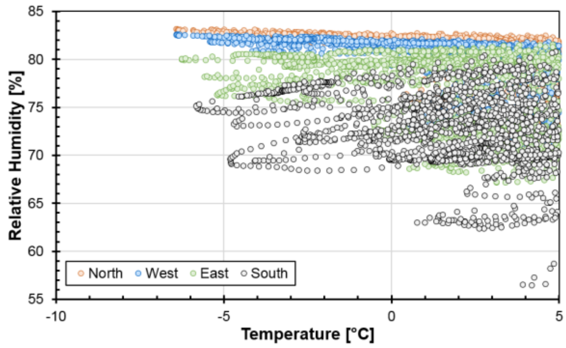

Fig. 47 Temperature and RH distribution under 5°C in the outermost MW insulation layer of a 44 cm masonry block depending on the orientation in BP

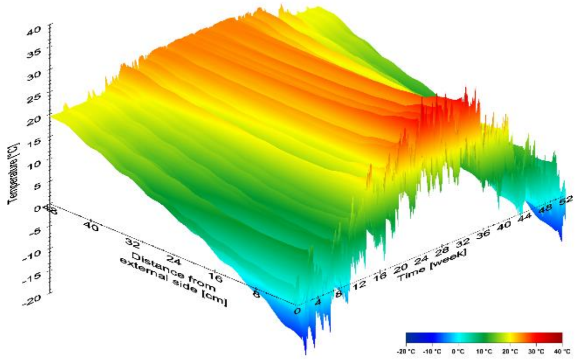

Fig. 48 Temperature distribution in north facing façade wall made of T44-MW filled masonry blocks obtained by using dynamic hygrothermal simulation

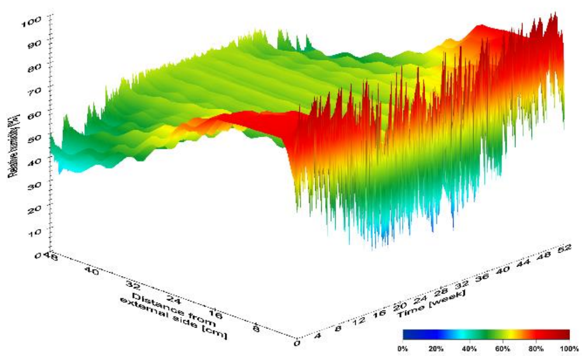

Fig. 49 Relative humidity distribution in north facing façade wall made of T44-MW filled masonry blocks obtained by using dynamic hygrothermal simulation

By using orientation-dependent 2D hygrothermal simulations on the walls made of masonry blocks filled by five different thermal insulations. At the moment of freezing, the moisture content of the thermal insulation is not critical (see **Fig. 48** and **Fig. 49)**, because the relative humidity is still in the hygroscopic regime in each cases. However, it should be noted, that in case of mineral wool insulations, there could be deterioration in the thermal [61] or mechanical properties [62] due to high relative humidity, when there are quality issues with the insulation. In **Fig. 50** and **Fig. 51**, I summarized the final results of the study. I showed, that the number of freeze-thaw cycles depend on the types of the thermal insulation as well as the orientation of the façade. The number of hours when the outermost insulation layer is under 0 °C also depends on the type of the filler material and on the orientation. According to the dynamic simulation results, during a 50 year designed service life of these type of blocks, the outermost insulating layer in PUR, EPS and EXP filled blocks has to withstand at least 900, MW has to withstand at least 1000, and AG has to withstand minimum 1100 freeze-thaw cycles; and there can be 348 and 500 hours frozen each year, depending on the insulation filler and orientation.

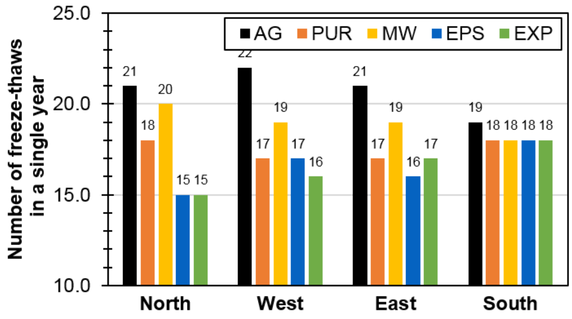

Fig. 50 Number of freeze-thaws in a single year

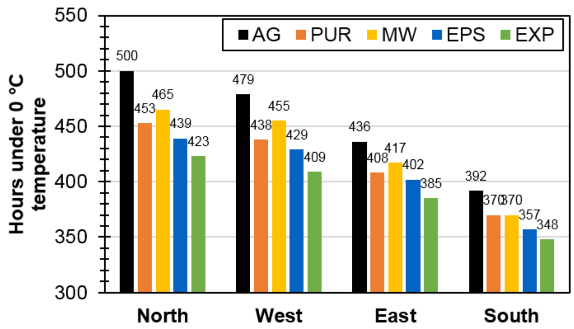

Fig. 51 Hours under zero degree Celsius temperature in a single year

Thesis 4: Durability and service life of insulation filled masonry blocks
Related publications: [NB4], [NB5], [NB7], [NB10]

I have showed, that in the case of 44 cm thick thermal insulation filled masonry blocks, the number of freeze-thaw cycles depend on the type of thermal insulation filler and the orientation of the façade. I have determined by dynamic hygrothermal simulations using climate data of Budapest, that during a 50 years designed service life, the outermost insulating layer in PUR foam, expanded polystyrene and expanded perlite filled blocks has to withstand at least 900, mineral wool has to withstand at least 1000, and aerogel blanket has to withstand minimum 1100 freeze-thaw cycles.

V. NUMERICAL OPTIMIZATION OF MODERN MASONRY BLOCKS

1. Optimization by the geometry of a selected insulation filled block

The optimized masonry block geometry is based on a mineral wool filled masonry block used as a starter block [63]. The geometry is shown in **Fig. 52**. The simulation model was simplified by neglecting the one tongue-and-groove connection on the sides shown in **Fig. 53**.

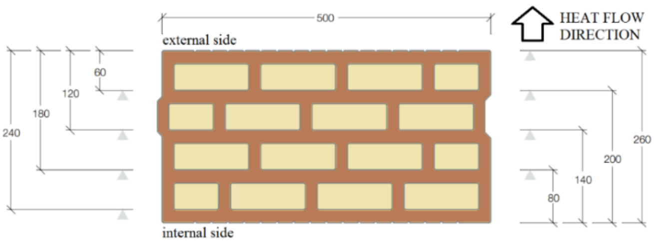

Fig. 52 Selected masonry block geometry

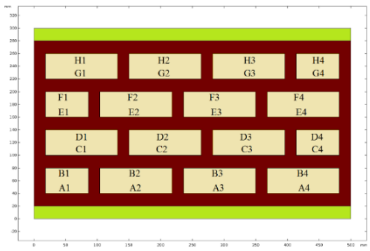

Fig. 53 Simplified geometry for optimization with marked variables

The initial hygrothermal simulation results are presented in **Fig. 54**. The U value of the initial masonry block calculated with **Table 3** material properties was U = 0.240 W/m^{2}K.

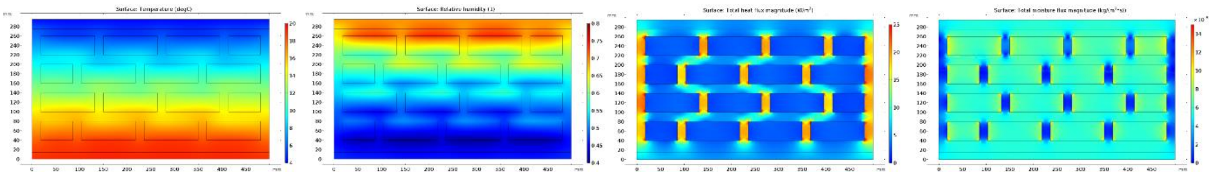

Fig. 54 Temperature, RH, heat and moisture flux distributions of the selected reference block

The optimization process was fully automated; the stepping was controlled by the COBYLA algorithm. In each step, a hygrothermal simulation was performed. **Fig. 55** shows how a result is developed from the initial geometry through the optimization steps. 6 different approach were presented in the dissertation to group and specify the variables, bounds and constraints.

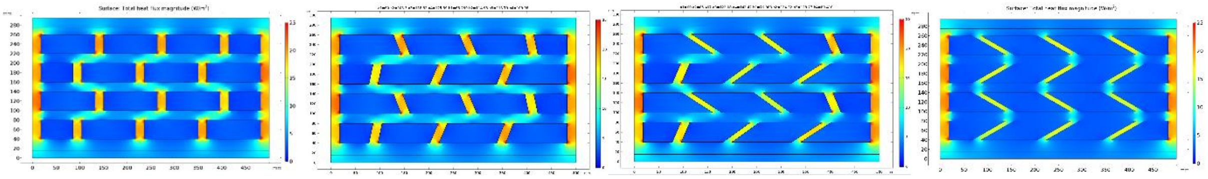

Fig. 55 Heat flux magnitudes of the initial, two intermediate and result geometry during optimization process

Excerpts of the optimized geometries are shown by **Fig. 56** and **Fig. 57**. In case of 6-ABBA, the U value obtained by using COBYLA optimization was as low as 0.193 W/m^{2}K.

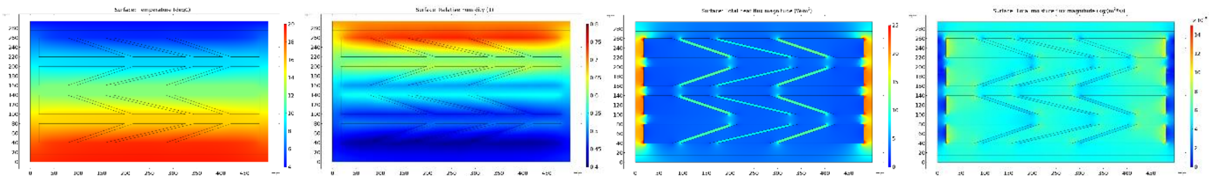

Fig. 56 Temperature, relative humidity, heat flux and moisture flux magnitudes of 3-ABAB

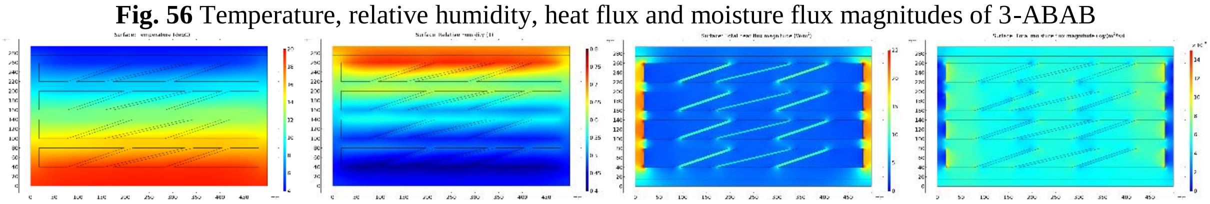

Fig. 57 Temperature, relative humidity, heat flux and moisture flux magnitudes of 6-ABBA

The results demonstrated that COBYLA algorithm is applicable to obtain lower U values of masonry blocks during an automatized optimization process. **Fig. 58** shows how many steps of optimization the algorithm needed to find the optimum and the achieved U values. It is clearly visible, that the selection of the variables and bounds has impact on the process time and number of optimization steps too.

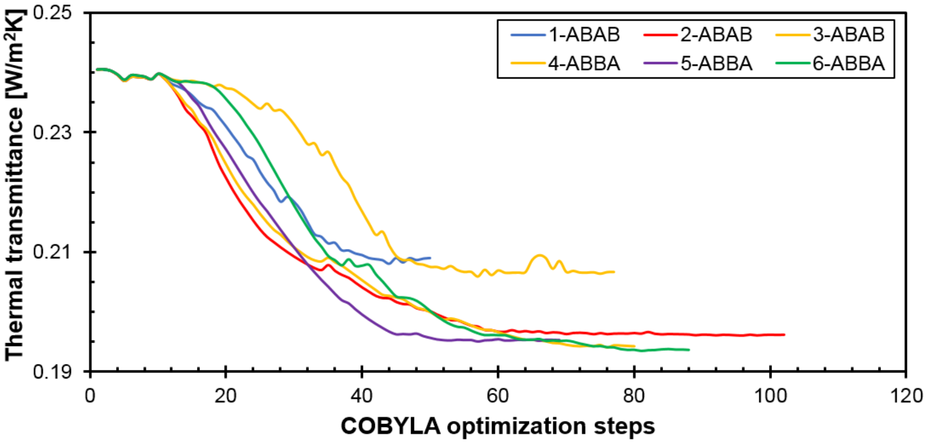

Fig. 58 Decrease of U value by COBYLA optimization steps

Thesis 5: Geometry optimization of an insulation filled masonry block
Related publications: [NB8]

Using hygrothermal simulations and COBYLA derivative-free numerical optimization with constraints, I have designed thermal insulation filled masonry blocks. I have showed that the masonry blocks designed by using numerical optimization outperform the initial reference blocks by up to 19.5%.

VII. THESES RELEATED PUBLICATIONS BY THE AUTHOR

[NB1] B. Nagy and M. Orosz, "Optimized Thermal Performance Design of Filled Ceramic Masonry Blocks," *Appl. Mech. Mater.*, vol. 797, pp. 174–181, 2015.

[NB2] B. Nagy, "Hőszigetelő anyagokkal töltött falazóblokkok többdimenziós kapcsolt hő - és nedvességtranszport vizsgálata," in *ÉPKÓ 2016*, 2016, pp. 182–185.

[NB3] B. Nagy, "Hőszigeteléssel töltött falazóblokkok laborvizsgálatokkal támogatott komplex modellezése," *Megtérülő Épületenergetika*, vol. 3, no. 3, pp. 22–26, 2016.

[NB4] B. Nagy and E. Tóth, "Hygrothermal behaviour of hollow and filled ceramic masonry blocks," in *International RILEM Conference on Materials, Systems and Structures in Civil Engineering 2016*, 2016, vol. 112, pp. 279–288.

[NB5] B. Nagy, "Hygrothermal modelling of masonry blocks filled with thermal insulation," in *MATEC Web of Conferences*, 2018, vol. 163.

[NB6] B. Nagy and G. Stocker, "Nedvességhidak az épületszerkezetekben," *Magy. Építőipar*, vol. 2018.5–6, pp. 168–171, 2018.

[NB7] B. Nagy and G. Stocker, "Hőszigeteléssel töltött falazóblokkok hőtechnikai és állagvédelmi vizsgálata," *Építési Hibák*, vol. 2018. december-január, pp. 9–14, 2018.

[NB8] B. Nagy, "Numerical Geometry Optimization and Modelling of Insulation Filled Masonry Blocks," *Lect. Notes Civ. Eng.*, vol. 20, no. NME 2018 issue, pp. 1–13, 2019.

[NB9] B. Nagy and G. Stocker, "Numerical Analysis of Thermal and Moisture Bridges in Insulation Filled Masonry Walls and Corner Joints," *Period. Polytech. Civ. Eng.*, under review

[NB10] B. Nagy, "Designing insulation filled masonry blocks against hygrothermal deterioration," *Eng. Fail. Anal.*, under review

[NB11] B. Nagy, "Multidimensional Hygrothermal Analysis of Complex Building Constructions," in *RILEM SPRING CONVENTION and SUSTAINABLE MATERIALS, SYSTEMS AND STRUCTURES CONFERENCE*, 2019. accepted

REFERENCES IN THE BOOK OF THESES

[1] Energy Information Administration, *International Energy Outlook 2016*. Energy Dept., Energy Information Administration, Office of Energy Analysis, 2016.
[2] D. J. C. Mackay, *Sustainable Energy - without the hot air*. UIT Cambridge Ltd., 2009.
[3] European Commission, “Roadmap 2050,” *Policy*, pp. 1–24, 2012.
[4] EPBD, “Energy Performance of Buildings Directive 2002/91/EU,” *Off. J. Eur. Union. Eur. Commision*, pp. 65–71, 2002.
[5] T. Horváth, “Épületenergetikai szabályozásunk körvonalai és előzményei,” *Magy. Építőipar*, vol. 67, no. 5, pp. 156–165, 2017.
[6] Z. Szalay, “The requirement system of the Hungarian directive on the energy performance of buildings,” *Period. Polytech. Archit.*, vol. 39, no. 2, p. 41, 2008.
[7] A. Zöld, Z. Szalay, and T. Csoknyai, *Energiatudatos Építészet 2.0*. TERC Kft., 2016.
[8] A. Aleksandra, F. Anagnostopoulos, F. Mariottini, and S. Kunkel, *Energy Performance Certificates Across the EU*. 2014.
[9] *176/2008. (VI. 30.) Korm. rendelet az épületek energetikai jellemz ő inek tanúsításáról*, no. 1. 2008.
[10] *7/2006. (V. 24) TNM rendelet, az épületek energetikai jellemzőinek meghatározásáról*, no. 1. 2018.
[11] European Parliament, “Direttiva 2010/31/UE del Parlamento europeo e del Consiglio, del 19 maggio 2010 , sulla prestazione energetica nell’edilizia,” *Off. J. Eur. Union*, vol. L153/13, no. 18.6.2010, pp. 13–35, 2010.
[12] A. et al. Arcipowska, “Energy Performance Certificates across Europe,” 2010.
[13] B. Nagy, “A Nemzeti Épületenergetikai Stratégia,” *Műszaki Ellenőr*, vol. 3, no. 1, pp. 44–46, 2014.
[14] Duna House Holding Nyrt., “Duna House Barométer,” *Duna House*, vol. 89, no. november, 2018.
[15] K. Severnyák and O. Fülöp, “ÉPÜLETEK ENERGETIKAI KÖVETELMÉNYEINEK KÖLTSÉGOPTIMALIZÁLT SZINTJÉNEK MEGÁLLAPÍTÁSÁT MEGALAPOZÓ SZÁMÍTÁSOK,” 2013.
[16] K. Severnyák, “Overhead Reduction or Energy Efficiency Measures,” *Appl. Mech. Mater.*, vol. 824, pp. 493–502, 2016.
[17] “Magyarország épület energetikai költségoptimalizálási vizsgálata - Jelentés az Európai Bizottság számára,” Budapest, 2018.
[18] A. Zöld and Z. Szalay, “Nearly Zero-Energy Requirements and the Reference Buildings,” *Adv. Mater. Res.*, vol. 899, pp. 52–57, Feb. 2014.
[19] Z. Szalay and A. Zöld, “Definition of nearly zero-energy building requirements based on a large building sample,” *Energy Policy*, vol. 74, pp. 510–521, Nov. 2014.
[20] M. Ferrara, V. Monetti, E. Fabrizio, M. Ferrara, V. Monetti, and E. Fabrizio, “Cost-Optimal Analysis for Nearly Zero Energy Buildings Design and Optimization: A Critical Review,” *Energies*, vol. 11, no. 6, p. 1478, Jun. 2018.
[21] K. Ahmed *et al.*, “A New Method for Contrasting Energy Performance and Near-Zero Energy Building Requirements in Different Climates and Countries,” *Energies*, vol. 11, no. 6, p. 1334, May 2018.
[22] E. Touloupaki, T. Theodosiou, E. Touloupaki, and T. Theodosiou, “Optimization of External Envelope Insulation Thickness: A Parametric Study,” *Energies*, vol. 10, no. 3, p. 270, Feb. 2017.
[23] B. Nagy, “Éghajlatfüggő tényezők pontosítása az épületenergetikai számításokban,” *ÉPÜLETGÉPÉSZ A Magy. ÉPŰLETGÉPÉSZEK SZÖVETSÉGÉNEK SZAKLAPJA*, vol. 1, no. 3, pp. 44–45, 2012.
[24] B. Nagy, D. Santos-Blastik, and G. Stocker, “A jövő otthona,” *Mérnök Újság*, vol. március, pp. 31–33, 2017.
[25] Z. Szalay, “AZ ÉPÜLETENERGETIKAI KÖVETELMÉNYEK VÁLTOZÁSAI ÉS VÁRHATÓ HATÁSUK A TÉGLA- ÉS CSERÉPIPARRA,” 2017.
[26] “Wienerberger.” [Online]. Available: https://wienerberger.hu/.
[27] “Leier.” [Online]. Available: https://www.leier.hu/kezdolap.
[28] H. Wang and Z. (John) Zhai, “Advances in building simulation and computational techniques: A review between 1987 and 2014,” *Energy Build.*, vol. 128, pp. 319–335, Sep. 2016.
[29] J. M. P. Q. Delgado, E. Barreira, N. M. M. Ramos, and V. P. de Freitas, *Hygrothermal Numerical Simulation Tools Applied to Building Physics*. Springer, 2013.
[30] J. Straube and E. Burnett, “Manual on Moisture Analysis in Buildings. Chapter 5: Overview of Hygrothermal (HAM) Analysis Methods,” in *ASTM manual 40-moisture analysis and condensation control in building envelopes*, H. R. Trechsel, Ed. Philadelphia, USA: ASTM International, 1991, pp. 81–89.
[31] I. Valovirta and J. Vinha, “Water Vapor Permeability and Thermal Conductivity as a Function of Temperature and Relative Humidity,” in *Performance of Exterior Envelopes of Whole Buildings, IX International Conference, Florida, USA, December 5-10, 2004*, 2004, p. 16.
[32] M. Jerman and R. Černý, “Effect of moisture content on heat and moisture transport and storage properties of thermal insulation materials,” *Energy Build.*, vol. 53, pp. 39–46, 2012.
[33] Á. Lakatos, “Moisture induced changes in the building physics parameters of insulation materials,” *Sci.*

Technol. Built Environ., vol. 22, no. 3, pp. 252–260, Apr. 2016.
[34] U. Berardi and M. Naldi, “The impact of the temperature dependent thermal conductivity of insulating materials on the effective building envelope performance,” *Energy Build.*, vol. 144, pp. 262–275, Jun. 2017.
[35] MSZ EN ISO 10456:2008, “Building materials and products. Hygrothermal properties. Tabulated design values and procedures for determining declared and design thermal values (ISO 10456:2007),” *Hungarian Stand. Inst.*, 2008.
[36] MSZ EN ISO 12571:2013, “Hygrothermal performance of building materials and products. Determination of hygroscopic sorption properties (ISO 12571:2013),” *Hungarian Stand. Inst.*, 2013.
[37] M. Krus and K. Kiessl, “Determination of the moisture storage characteristics of porous capillary active materials,” *Mater. Struct.*, vol. 31, no. 8, pp. 522–529, Oct. 1998.
[38] MSZ EN 1936:2007, “Natural stone test methods. Determination of real density and apparent density, and of total and open porosity,” *Hungarian Stand. Inst.*, 2007.
[39] MSZ EN ISO 12572:2016, “Hygrothermal performance of building materials and products. Determination of water vapour transmission properties. Cup method (ISO 12572:2016),” *Hungarian Stand. Inst.*, 2016.
[40] M. Krus and A. Holm, “Simple Methods To Approximate the Liquid Transport Coefficients Describing the,” *5th Symp. ‘Building Phys. Nord. Countries’, Göteborg*, pp. 241–248, 1999.
[41] MSZ EN ISO 12570:2000, “Hygrothermal performance of building materials and products. Determination of moisture content by drying at elevated temperature (ISO 12570:2000),” *Hungarian Stand. Inst.*, 2000.
[42] MSZ EN 1602:2013, “Thermal insulating products for building applications. Determination of the apparent density,” *Hungarian Stand. Inst.*, 2013.
[43] F. Fülöp and E. Tátrainé Szekeres, “Calorimetric measurements - Measurement of heat capacity,” Budapest University of Technology and Economics, 2014.
[44] Z. Pavlik, J. Pavlik, M. Jirickova, and R. Cerny, “System for Testing the Hygrothermal Performance of Multi-Layered Building Envelopes,” *J. Therm. Envel. Build. Sci.*, vol. 25, no. 3, pp. 239–249, Jan. 2002.
[45] Ahlborn Mess- und Regelungstechnik GmbH, “Ahlborn ALMEMO® system.” [Online]. Available: https://www.ahlborn.com/en_UK/almemo.
[46] W. Frei, “Optimization with COMSOL Multiphysics,” *COMSOL Tokyo Conf. 2014*, pp. 1–55, 2014.
[47] J. M. Hammersley and D. C. Handscomb, “General Principles of the Monte Carlo Method,” in *Monte Carlo Methods*, Dordrecht: Springer, 1964, pp. 50–75.
[48] J. A. Nelder and R. Mead, “A Simplex Method for Function Minimization,” *Comput. J.*, vol. 7, no. 4, pp. 308–313, Jan. 1965.
[49] M. J. D. Powell, “A Direct Search Optimization Method That Models the Objective and Constraint Functions by Linear Interpolation,” in *Advances in Optimization and Numerical Analysis*, Dordrecht: Springer Netherlands, 1994, pp. 51–67.
[50] M. Powell, “A view of algorithms for optimization without derivatives,” *Math. Today-Bulletin Inst. …*, pp. 1–12, 2007.
[51] Ansys Inc., “Ansys Mechanical.” .
[52] S. Fantucci and V. Serra, “Thermal effectiveness of low emissivity coatings in hollow bricks : a numerical analysis for different cavity concentration,” *Int. Mason. Conf. 2014*, no. December, pp. 1–11, 2014.
[53] M. Arici, B. Yılmaz, and H. Karabay, “Investigation of Heat Insulation Performance of Hollow Clay Bricks Filled with Perlite,” *ACTA Phys. Pol. A*, vol. 130, no. 1, pp. 266–268, 2016.
[54] T. GmbH, “Testo 885-2.” [Online]. Available: https://www.testo.com/en-AU/testo-885-2-kit/p/0563-0885-V3.
[55] Amphenol Corporation, “Protimeter MMS2.” [Online]. Available: https://www.amphenol-sensors.com/microsites/protimeter/MMS2.
[56] MSZ EN 1745:2012, “Masonry and masonry products. Methods for determining thermal properties,” *Hungarian Stand. Inst.*, 2012.
[57] G. S. LLC, “Surfer.” [Online]. Available: https://www.goldensoftware.com/products/surfer.
[58] Meteotest, “Meteonorm 7.” [Online]. Available: https://meteonorm.com/en/.
[59] MSZ EN 15026:2007, “Hygrothermal performance of building components and building elements. Assessment of moisture transfer by numerical simulation,” *Hungarian Stand. Inst.*, 2007.
[60] MSZ EN ISO 6946:2017, “Building components and building elements. Thermal resistance and thermal transmittance. Calculation methods (ISO 6946:2017),” *Hungarian Stand. Inst.*, 2017.
[61] B. Nagy and T. K. Simon, “Energy and hygrothermal performance of builtin mineral wool thermal insulations,” in *MATEC Web of Conferences*, 2018, vol. 163, p. 8.
[62] T. K. Simon, L. Mlinárik, and V. Vargha, “Effect of water vapor on the compressive strength of a mineral wool insulation board,” *J. Build. Phys.*, vol. 39, no. 3, pp. 285–294, Nov. 2015.
[63] Wienerberger, *Porotherm W.i Objekt Plan*. 2017.